Microchemical Journal 193 (2023) 109142

Contents lists available at ScienceDirect

Microchemical Journal

journal homepage: www.elsevier.com/locate/microc

The development, validation, and optimization of a SWAdSV method for the simultaneous determination of epinephrine and uric acid in real samples using a poly(L-cysteine) modified SPCE sensor

David Majer, Matjaž Finšgar *

University of Maribor, Faculty of Chemistry and Chemical Engineering, Smetanova ulica 17, 2000 Maribor, Slovenia

ARTICLE INFO

Keywords:
Epinephrine
Uric acid
L-cysteine
pLC-SPCE
ToF-SIMS

ABSTRACT

This work demonstrates the development, optimization, and method validation of a square-wave adsorption stripping voltammetry (SWAdSV) method for the simultaneous determination of epinephrine (EP) and uric acid (UA) using a poly(L-cysteine) (pLC) film modified screen-printed carbon electrode (pLC-SPCE). The pLC film was deposited by the electropolymerization of L-cysteine (LC). The successful deposition of pLC was confirmed by time-of-flight secondary ion mass spectrometry. A comparison was made between a bare SPCE and a pLC-SPCE for the analysis of EP and UA. In order to improve the electroanalytical performance of the pLC-SPCE sensor, the parameters of the square-wave (SW) technique, such as amplitude, frequency, and potential step, as well as the pH of the 0.1 M PBS solution, the concentration of the LC, the number of cycles for electropolymerization, the deposition potential, and the deposition time, were optimized. Subsequently, the SWAdSV method was validated for the limit of detection (LOD), the limit of quantification (LOQ), the linear concentration range, accuracy, and precision. The method had a very low LOD and LOQ, i.e. 10.0 μg/L and 19.8 μg/L for both analytes, respectively. Two linear concentration ranges were obtained, i.e. from 49.0 μg/L to 326.1 μg/L and from 326.1 μg/L to 887.1 μg/L, for both analytes. The average recoveries and the relative standard deviations for both analytes were in a range from 94.4% to 108.4% ($n = 6$) and from 2.6% to 11.7% ($n = 6$), respectively, at the four EP and UA concentration levels tested. In addition, the effect of possible interferents, such as glucose, L-ascorbic acid, K^+, Cl^-, Ca^{2+}, SO_4^{2-}, Mg^{2+}, NH_4^+, $C_2O_4^{2-}$, and urea on the SW signal of EP and UA, were investigated. However, none of these compounds significantly affected the performance of the electroanalytical method. Finally, the applicability of the pLC-SPCE sensor was successfully demonstrated for the analysis of a pharmaceutical sample (an EP auto–injector) and human urine, proving accurate and precise analysis using the developed sensor.

1. Introduction

Epinephrine (EP) is a hormone and neurotransmitter produced by the adrenal gland. Deviations from normal epinephrine concentrations in the human body are associated with Parkinson's disease, Huntington's disease, hypoglycemia, chronic active hepatitis, etc. [1]. EP undergoes multiple metabolic pathways, including oxidation, conjugation, and deamination, leaving only a tiny percentage of EP unchanged in human urine. Therefore, the determination of EP in human urine requires a selective method with a low limit of detection (LOD) [2]. On the other hand, EP is used for various medical purposes, such as cardiac arrest, sepsis, bronchial conditions, asthma management, and anaphylaxis treatment [3]. Anaphylaxis is a severe and potentially life-threatening allergic reaction characterized by the acute onset of symptoms involving different organ systems and requiring immediate medical attention [4]. Anaphylactic reactions are treated with EP using an EP auto-injector [5]. The dosage of EP for the treatment of anaphylaxis varies between adults and children or may be body–weight–dependent, emphasizing the importance of an accurate concentration of EP in auto–injectors [6].

Uric acid (UA) is a breakdown product of endogenous (adenine and guanine in DNA and RNA) or exogenous (food) purines [7]. It is important to maintain normal levels of UA in the blood as both high and low levels can have severe effects on human health. Low UA levels are associated with Alzheimer's disease and Parkinson's disease, whereas high levels can cause Lesch-Nyhan syndrome, hyperuricemia, gout, etc

* Corresponding author.
E-mail address: matjaz.finsgar@um.si (M. Finšgar).

https://doi.org/10.1016/j.microc.2023.109142
Received 21 June 2023; Received in revised form 24 July 2023; Accepted 25 July 2023
Available online 27 July 2023
0026-265X/© 2023 The Author(s). Published by Elsevier B.V. This is an open access article under the CC BY-NC-ND license (http://creativecommons.org/licenses/by-nc-nd/4.0/).

[8]. UA is mainly formed in the liver and excreted through the kidneys in the urine. The typical UA concentration in human urine for a healthy individual ranges from 235.5 mg/L to 738.7 mg/L [9].

The analysis of EP and UA is usually performed by gas chromatography (GC) [10,11], high performance liquid chromatography (HPLC) [12,13], spectrophotometry [14,15], and capillary electrophoresis [16,17]. While GC and HPLC offer high accuracy, precision, and selectivity, they also suffer from many drawbacks such as time-consuming analysis, the use of environmentally unfriendly organic solvents, and the need for extensive sample pretreatment [18,19].

In contrast, electroanalytical methods outperform these techniques in several aspects. They offer fast analysis time, low LODs, cost-effective equipment (significantly lower compare to chromatography), the ability to perform on-site analysis, minimal sample pretreatment, and the advantage of using water as a solvent, which is in accordance with the guidelines of modern chemistry [20]. Among the electroanalytical methods, square-wave voltammetry (SWV) is widely used because of its short analysis time, high sensitivity, and low LODs [21].

Screen-printed carbon electrodes (SPCEs) have gained significant attention in electroanalytical instrumentation in recent years due to their portability, low-cost, low background currents, miniaturization, and disposability [22]. However, the primary limitation of using an unmodified SPCE (referred to as a bare SPCE) for the individual or simultaneous analysis of EP and UA is their inability to detect EP in the presence of UA (or L-ascorbic acid, L-AA) and vice versa [23]. This interference arises from their similar oxidation peak potentials (E_p) and slow electron kinetics, resulting in an overlap of voltammetric peaks. Additionally, the LODs for both analytes are high [24]. Consequently, developing a selective method for EP in UA determination with low LODs and high accuracy and precision poses a real challenge. In order to overcome these challenges, the surface of the SPCE working electrode (WE) can be effectively modified with various modifiers, such as carbon nanotubes [25], nanocomposites or nanoparticles [26], polymers [27], etc. WE modification thereby plays a crucial role in lowering the LODs and separating the oxidation E_p of different analytes, thereby improving selectivity [28].

Amino acids have been used as effective WE modifiers due to their excellent physical and chemical characteristics, such as high conductivity, stability, and ease of preparation [29]. Among them, L-cysteine, a non-essential amino acid, can be utilized as a promising WE modifier. With its amino, sulfhydryl, and carboxyl functional groups, L-cysteine can be electropolymerized to form a poly(L-cysteine) (pLC) film on the WE surface. This film enhances the conductivity, stability, and selectivity of the electrode, improving its overall performance [30].

In electroanalysis, parameters such as the pH of the supporting electrolyte, the concentration of the modifier, the accumulation time, deposition potential, etc., are commonly optimized [31].

Few research studies have been published on the simultaneous determination of EP and UA on a modified WE, such as a glassy carbon electrode (GCE). For example, Kalimuthu and John [32] developed a method for the simultaneous determination of EP, UA, and xanthine in the presence of ascorbic acid (AA). The surface of the GCE was modified with an ultrathin polymer film of 5–amino–1,3,4–thiadiazole–2-thiol. In another study, Ghanbari and Hajian [33] modified GCE with a Au/ZnO/PPy/RGO nanocomposite and used it for the simultaneous determination of EP, UA, and AA.

However, to the best of our knowledge, no work has been published on the simultaneous determination of EP and UA using a modified SPCE.

In this work, a new square-wave adsorptive stripping voltammetry (SWAdSV) method for the simultaneous determination of EP and UA was developed. The surface of the SPCE sensor was modified with pLC film (pLC-SPCE). Successful deposition was confirmed using time-of-flight secondary ion mass spectrometry (ToF-SIMS). The development process involved the optimization of several parameters. This was crucial to achieving the best electroanalytical performance of the pLC–SPCE sensor. The developed pLC-SPCE sensor has demonstrated its applicability for the simultaneous determination of EP and UA in an EP auto-injector and human urine.

2. Experimental

2.1. Apparatus and SPCE sensors

The electrochemical measurements in this study were conducted using a PalmSens 4 potentiostat/galvanostat (PalmSens, Houten, The Netherlands) under controlled laboratory conditions at 22 °C ± 2 °C. The PalmSens 4 was operated with PSTrace 5.9 software.

As a three-electrode system, SPCE sensors of type AC1.W4.R2 with batch number 21128 were supplied by BVT Technologies (Brno, Czech Republic). These SPCE sensors consist of the WE and a counter electrode, both made of carbon, with a 1 mm diameter for the WE. The reference electrode (RE) was made of Ag coated with AgCl for enhanced stability. All potentials (E) in this work are reported as E vs. this RE electrode. All three electrodes are printed on the same alumina ceramic substrate.

2.2. Reagents and solutions

$Na_2HPO_4{\cdot}7H_2O$ (purity ≥ 99 wt.%), $NaH_2PO_4{\cdot}H_2O$ (purity ≥ 98 wt.%), $MgCl_2{\cdot}6H_2O$ (purity 99 wt.%), and $CaCl_2$ (ACS reagent) were supplied by Acros Organics (Fair Lawn, NJ, USA). NaOH (Analytical Reagent, Reag. ACS, Reag. Ph. Eur.) was supplied by Sigma-Aldrich Laborchemikalien GmbH (Seelze, Germany). H_3PO_4 (85%) was supplied by Lach:ner (Neratovice, Czech Republic). NH_4I (purity ≥ 99 wt.%, ACS reagent), urea (purity ≥ 98 wt.%, BioReagent), Na_2SO_4 (purity ≥ 99.99 wt.%, trace metals basis), L–cysteine hydrochloride (anhydrous, purity ≥ 98 wt.%), UA (purity ≥ 99 wt.%), and sodium oxalate (purity ≥ 99.5 wt.%, ACS reagent) were supplied by Sigma Aldrich (St. Louis, MO, USA). KCl (purity ≥ 99.5 wt.%, for analysis) and NaCl (purity ≥ 99.5 wt.%, for analysis, ACS, ISO, Reag. Ph. Eur.) were supplied by Merck (Darmstadt, Germany). L-AA (for analysis-ISO) was supplied by Carlo Erba Reagents (Val de Reuil, France). H_2SO_4 (95–97 vol.%) and anhydrous ethanol (Ph. Eur.) was supplied by Kefo (Ljubljana, Slovenia). D-glucose anhydrous (analytical grade reagent) was supplied by Fisher Scientific (Loughborough, Leicestershire, UK). The USP reference standard EP bitartrate (purity 99.9 wt.%) was supplied by Sigma Aldrich (Rockville, MD, USA). For the method optimization, method validation, and real sample analysis, the solutions of EP and UA standard were prepared in 0.1 M phosphate buffer solution (PBS) with a pH of 4.50, which served as a supporting electrolyte. When necessary, the EP and UA solutions were prepared in 0.1 M PBS with a pH ranging from 2.00 to 10.00. The 0.1 M PBS was prepared using ultra-pure water with a resistivity of 18.2 MΩ cm, produced by the ELGA water purification system (Lane End, UK).

2.3. Square-wave adsorptive stripping voltammetry

In order to obtain optimized SWAdSV parameters such as E_{dep}, deposition time (t_{dep}), amplitude, E step (E_{step}), and frequency, these parameters were changed, and the SWAdSV response was measured. For the optimization of amplitude, E_{step}, and frequency, the E range was from −0.600 V to 0.600 V.

Method optimization, method validation, and real sample analysis were performed using SWAdSV. Prior to each SWAdSV measurement during method validation and real sample analysis, the deposition potential (E_{dep}) was applied at 0.000 V for 15 s (this E_{dep} was deemed to be optimal, as explained below), followed by a 5 s equilibration time. The SWAdSV measurement was performed in an E range from −0.100 V to 0.400 V with a positive-going E sweep. The optimal amplitude of 0.010 V, optimal E_{step} of 0.010 V, and optimal frequency of 10 Hz were employed (optimization is explained below). During the E_{dep}, the electrochemical cell was stirred with a magnetic stirrer and a magnetic stirring bar. The SWAdS voltammogram measurement lasted

approximately 5 s. After multiple uses of pLC-SPCE, the surface was rinsed with a 50 vol.% ethanol/50 vol.% ultrapure water solution to remove any remaining EP and UA residuals before the subsequent analysis.

2.4. Cyclic voltammetry

Cyclic voltammetry (CV) was used to condition freshly employed SPCE sensors and deposit LC on the surface of the WE. Conditioning was performed by immersing the SPCE sensor in 0.5 M H_2SO_4. The CV measurement started at a starting E (E_s) of −1.500 V. The E was swept toward a more positive E until a switching E (E_{sw}) of 1.500 V was reached. The E was then reversed until reaching a final E (E_f) of −1.500 V. A sweep rate (ν) of 100 mV/s and E_{step} of 0.010 V were employed for 10 consecutive cycles.

2.5. pLC-SPCE sensor preparation

After being conditioned in 0.5 M H_2SO_4, the conditioned SPCE sensor was rinsed with ultra-pure water to remove any remaining H_2SO_4, and the excess water was soaked up with a chemically inert wipe (Kimtech, Reigate, UK) without touching the surface of WE. Subsequently, the conditioned SPCE sensor was immersed in an electrochemical cell containing 0.1 M PBS solution with a pH of 7.00, which contained 2 mM of LC. The deposition was performed using CV with the following parameters: an E_s of −1.000 V, an E_{sw} of 2.000 V, an E_f of −1.000 V, E_{step} of 0.010 V, a ν of 100 mV/s, and 10 cycles. After deposition, the obtained pLC-SPCE sensor was rinsed with a 50 vol.% ethanol/50 vol.% ultrapure water solution, followed by rinsing with ultrapure water to wash off the residues of LC and ethanol. The remaining water on the sensor was again soaked up with a chemically inert wipe. The pLC-SPCE sensor was then electroactivated using SWV.

For method optimization, the number of cycles and the concentration of LC were different compared with those given above.

2.6. Optimization

In order to achieve the best electroanalytical performance of the pLC-SPCE sensor, optimization was performed. The best electroanalytical performance was considered in terms of maximizing the peak-to-peak separation between the E_P of EP (E_p^{EP}) and UA (E_p^{UA}) ($\left|E_p^{EP} - E_p^{UA}\right|$) while maintaining the ratio ($\Delta i_p^{EP}/\Delta i_p^{UA}$) between the peak height for EP (Δi_p^{EP}) and UA (Δi_p^{UA}) close to 1. In addition, the increase of the Δi_p^{EP} and Δi_p^{UA} was also considered. To achieve this, several parameters were optimized, including amplitude, E_{step}, frequency, the pH of the 0.1 M PBS solution, the LC concentration for electropolymerization, the number of cycles during electropolymerization, E_{dep}, and t_{dep}. However, it is important to note that for certain parameters, different criteria were selected based on their specific impact on the overall performance of the pLC-SPCE sensor. With such a systematic approach to optimizing every parameter, it was possible to improve the initial electroactive performance of the pLC-SPCE sensor, which was useful for the real sample analysis.

2.7. ToF-SIMS

Surface analysis of the developed pLC-SPCE sensor was performed using ToF-SIMS. ToF-SIMS measurements were conducted using an M6 device (IONTOF, Münster, Germany). Bi_3^+ was used as a primary beam with a target current of 0.6 pA. The calibration of the measured spectra in both polarities (positive and negative) was performed by referencing known peaks at a certain mass-to-charge (m/z) ratio. Positive ion spectra were calibrated using peaks at m/z 15.02 for CH_3^+, m/z 27.02 for $C_2H_5^+$, m/z 43.05 for $C_3H_7^+$, m/z 53.04 for $C_4H_5^+$, m/z 57.07 for $C_4H_9^+$, and m/z 69.07 for $C_5H_9^+$. Negative ion spectra were calibrated using peaks at m/z 24.00 for C_2^-, m/z 36.00 for C_3^-, m/z 48.00 for C_4^-, and m/z 60.00 for C_5^-. The data were acquired and processed using SurfaceLab 7.3 software (IONTOF, Münster, Germany). The pLC-SPCE sensor was dried under a stream of nitrogen gas before transfer to the pre–chamber of the ToF-SIMS device. The pressure in the sample analysis chamber was in the range of 10^{-11} mbar.

2.8. Real sample analysis

The content of EP and UA in EP an auto-injector and human urine were determined. Both real samples were analysed without sample pretreatment. Measurements were performed in 0.1 M PBS solution with a pH of 4.50. To check the accuracy and precision of the obtained results, the samples were spiked with a solution of a known amount of EP or UA standard.

3. Results and discussion

3.1. Electropolymerization of the LC and pLC-SPCE sensor activation

The electropolymerization of LC on the SPCE surface was successfully achieved using CV. Fig. S1 (in Supplementary Information) shows the cyclic voltammograms obtained during the electropolymerization process of 2 mM LC at a ν of 100 mV/s in 0.1 M PBS with a pH of 7.00. Despite the fact that the electropolymerization of LC has been previously reported using different electrodes, such as GCE [34], this work employed a similar procedure with a slight modification in the potential E range. To the best of our knowledge, this study represents the first successful electropolymerization of L-cysteine on a bare SPCE sensor. Furthermore, there was no need for additional modifications involving different nanoparticles, such as Au nanoparticles [35–37], which are typically used for L-cysteine modification.

An E sweep to more positive E (the anodic direction) results in two oxidation peaks at approximately 0.400 V and 1.500 V (Fig. S1). The oxidation peak at 0.400 V corresponds to the oxidation of the sulfhydryl group (-SH), which resulted in a radical formation (·RS). Subsequently, radical coupling occurs, resulting in the formation of L-cystine. The oxidation peak at 1.500 V corresponds to the oxidation of L-cystine to L-cysteic acid (Fig. S1) [38].

The developed pLC-SPCE sensor was characterized by the ToF-SIMS technique to confirm the successful deposition of LC on the WE in the form of pLC film. The presence of SO_3H^- at m/z 80.97 (Fig. 1a), SH^- at m/z 32.98 (Fig. 1b), and NH_2^+ at m/z 16.02 (Fig. 1c) were confirmed on the surface of the pLC-SPCE sensor. These two functional groups are crucial for the formation of pLC film and the adsorption of pLC film on the surface of the SPCE sensor [38]. Additionally, SO_3^- at m/z 79.96 (resulting from the loss of one hydrogen atom from SO_3H^-, Fig. S2a), S^- at m/z 31.97 (Fig. S2b), and COO^- at m/z 43.99 (Fig. S2c) were also present in the negative ion ToF-SIMS spectra. These fragments correspond to LC (NH_2^+, SH^-, S^-, and COO^-) and to the products of LC electropolymerization, such as L-cysteic acid (NH_2^+, SO_3H^-, SO_3^-, S^-, and COO^-). The presence of L–cysteic acid is consistent with the CV voltammogram of LC electropolymerization, where L-cysteic acid was formed at an E of 1.500 V (Fig. S1).

The pLC-SPCE sensor was also analysed using ToF-SIMS after applying an E_{dep} of 0.000 V for 15 s in 0.1 M PBS (pH = 4.50) containing 1.0 mg/L of EP and UA. The presence of pLC film was also confirmed, as the same fragments as mentioned above were present. In addition, $C_9H_{13}NO_3^+$ (the parent ion of EP) at m/z 183.08 (Fig. S2d) and $C_9H_{14}NO_3^+$ (the parent ion of EP after the addition of one hydrogen atom) at m/z 184.09 (Fig. S2e) were found on the surface. On the other hand, no parent ion corresponding to UA was found on the pLC-SPCE after applying the E_{dep}. This suggests that only EP is adsorbed on the surface of the pLC-SPCE after the E_{dep} is applied.

The obtained pLC-SPCE sensor had to be electroactivated due to the

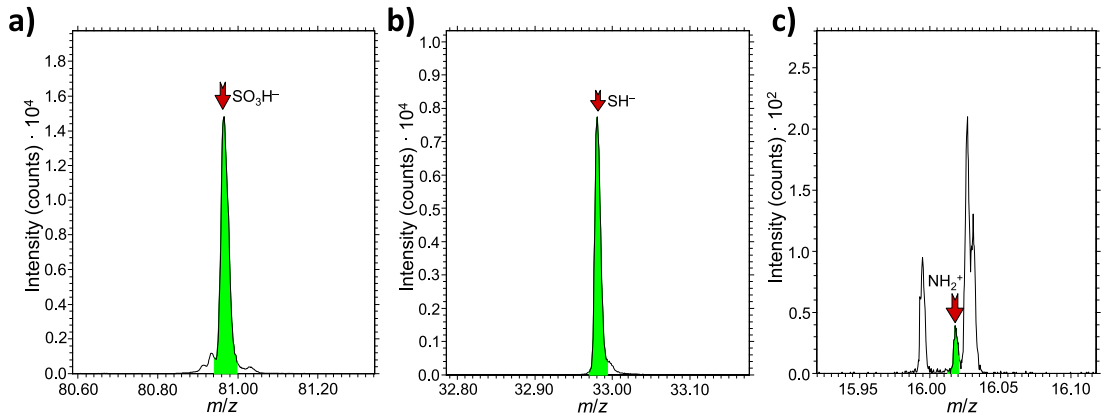

Fig. 1. ToF-SIMS spectra measured in the negative polarity for a) SO_3H^- at *m/z* 80.97 and b) SH^- at *m/z* 32.98, and the TOF–SIMS spectrum measured in the positive polarity for c) NH_2^+ at *m/z* 16.02.

baseline changes of sequentially measured SW voltammograms in 0.1 M PBS with a pH of 4.50 (Fig. 2). Fig. 2a shows that the baseline of the 1st sweep in the SW voltammogram started to increase significantly in an *E* range from −0.200 V to 0.600 V. However, with the 2nd sweep, the baseline stabilized (the intensity was significantly lower in that *E* range compared to the 1st sweep) and the intensity decreased further with consecutive sweeps (Fig. 2a). To activate the pLC-SPCE, it was essential to develop a method with a stable baseline. It was found that 10 consecutive sweeps in 0.1 M PBS (pH = 4.50) in an *E* range from −0.600 V to 0.600 V were necessary to obtain a stable baseline. During each sweep, the electrochemical cell was stirred for 15 s followed by a 5 s equilibration time. Fig. 2b shows the 1st, 9th, and 10th sweeps, with the 9th and 10th sweeps completely overlapping. After the 10th consecutive sweep, the *E* range for SWAdSV measurements was narrowed from an *E* range of −0.600 V to 0.600 V to an *E* range of −0.100 V to 0.400 V, since the oxidation peaks for EP and UA develop at *E* more negative than 0.400 V (Fig. 2c). This *E* range from −0.100 V to 0.400 V was then used for the optimization of E_{dep}, t_{dep}, method validation, and real sample analysis.

The reason for the required electroactivation of pLC-SPCE could be the changes in the surface of the prepared pLC-SPCE sensor and, thus, the capacitance. With each sweep, the surface of the LCA–SPCE changes, leading to variations in capacitance until it stabilizes after 10 sweeps [18].

A comparison was made between the bare SPCE and pLC-SPCE sensors to assess their electroanalytical performance for the analysis of EP and UA. A solution of EP and UA standards was measured at a mass concentration (γ) of 200.1 μg/L for both sensors. The oxidation peaks for EP and UA completely overlapped on the bare SPCE (Fig. 3a) and were not well shaped (not developed) at such low EP and UA concentrations, which is consistent with the relatively high LODs for both analytes on bare SPCE sensors reported previously [39]. On the other hand, two well–defined and separated oxidations peaks for EP and UA were obtained using the pLC-SPCE (Fig. 3b). Moreover, the peak heights (Δi_p) for both analytes at a concentration of 200.1 μg/L were significantly higher than the Δi_p of the peaks that overlap on the bare SPCE. This indicates that the presence of pLC film on the surface of the SPCE sensor improves peak-to-peak separation and increases the signal for EP and UA.

3.2. *The effects of changing LC concentrations and the number of cycles on the electroanalytical performance of the pLC–SPCE sensor*

The effects of the LC concentration and the number of cycles were optimized to achieve the best electroanalytical performance of the pLC-SCPE sensor. All measurements were performed in triplicate in 0.1 M PBS (pH = 4.50) containing 1.0 mg/L of EP and UA. The thickness of the film can be controlled by the concentration of the modifier (LC in this work) and the number of cycles. If the film is too thin, it will not have enough active sites, while a very thick film will tend to block electron transfer [34]. Thus, it is essential to determine the optimal LC concentration and the number of cycles that yield the highest Δi_p^{EP} and Δi_p^{UA} values.

To optimize the LC concentration, solutions ranging from 0.5 mM to 3.0 mM of LC were prepared in 0.1 M PBS with a pH of 7.00. The Δi_p for both analytes increased with increasing LC concentration from 0.5 mM to 2 mM (Fig. S3a,b). With an increase in LC concentration higher than

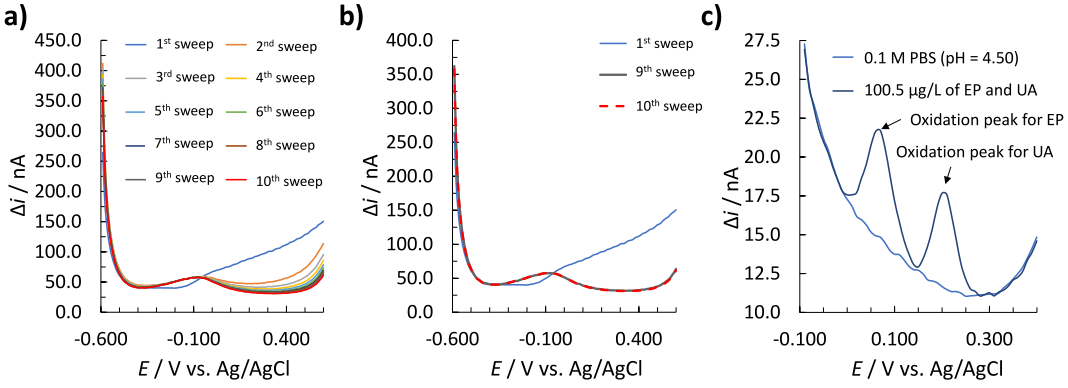

Fig. 2. a) Electroactivation of the pLC-SPCE sensor using a SWV, where 10 consecutive sweeps were performed in 0.1 M PBS (pH = 4.50 in an *E* range from −0.600 V to 0.600 V, b) SW voltammograms of the 1st, 9th, and 10th consecutive sweeps (note that the 9th and 10th sweeps completely overlap), and c) SWAdS voltammograms measured in 0.1 M PBS (pH = 4.50) containing 100.5 μg/L of EP and UA in an *E* range from −0.100 V to 0.400 V.

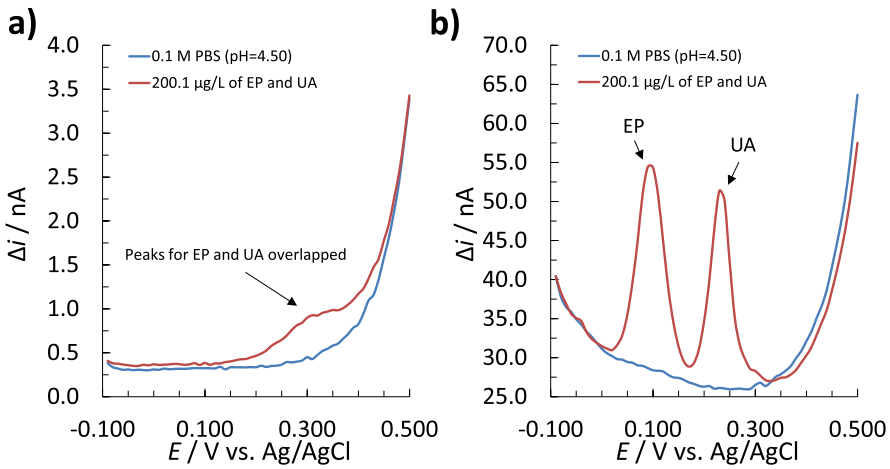

Fig. 3. SWAdS voltammograms measured in 0.1 M PBS (pH = 4.50) and in 0.1 M PBS (pH = 4.50) containing 200.1 µg/L of EP and UA measured with a) the bare SPCE and b) the pLC-SPCE.

2.0 mM, the Δi_p started to decrease, possibly due to the excessive thickness of the polymer film on the WE surface, which increases resistivity and blocks electron transfer [37] (Fig. S3a,b). Therefore, an LC concentration of 2 mM was selected as the optimal concentration for the next optimization procedure.

In order to optimize the number of cycles, a 2 mM LC solution in 0.1 M PBS (pH = 7.00) was electropolymerized using various numbers of cycles, ranging from 1 to 25. The highest Δi_p^{EP} was obtained after 10 cycles (Fig. S3c), while the highest Δi_p^{UA} was obtained after 15 cycles (Fig. S3d). Since the highest Δi_p for both analytes was not obtained with the same number of cycles, the wider $\left|E_p^{EP} - E_p^{UA}\right|$ and the $\Delta i_p^{EP}/\Delta i_p^{UA}$ closest to 1 were considered. However, the widest $\left|E_p^{EP} - E_p^{UA}\right|$ was observed for 15 cycles (Fig. S3e), whereas the $\Delta i_p^{EP}/\Delta i_p^{UA}$ closest to 1 was obtained at 10 cycles (Fig. S3f). In this case, 10 cycles was selected as the optimal value for the next optimizazion procedure compared to 15, as it shortens the electropolymerization process.

3.3. The effect of changing SW parameters on the electroanalytical performance of the pLC-SPCE sensor

The optimization of SW parameters to obtain better electroanalytical performance of the pLC–SPCE sensor was performed. The SW parameters for optimization were amplitude, frequency, and E_{step}. The optimal parameters were considered to be those exhibiting the widest $\left|E_p^{EP} - E_p^{UA}\right|$, while maintaining the $\Delta i_p^{EP}/\Delta i_p^{UA}$ close to 1. A wide $\left|E_p^{EP} - E_p^{UA}\right|$ is critical to minimizing the overlap between the peaks and achieving the desired resolution. In addition, maintaining the $\Delta i_p^{EP}/\Delta i_p^{UA}$ close to 1 in the optimization procedure ensures that one component does not significantly affect the other one. All measurements were performed in triplicate in 0.1 M PBS (pH = 7.00) containing 1.0 mg/L of EP and UA.

The following amplitude values were employed: 0.001 V, 0.010 V, 0.020 V, 0.030 V, 0.040 V, and 0.050 V (Fig. S4c). The widest $\left|E_p^{EP} - E_p^{UA}\right|$ and the $\Delta i_p^{EP}/\Delta i_p^{UA}$ closest to 1 were determined at an amplitude of 0.010 V (Fig. S4a,b). It should be noted that when the amplitude was set at 0.001 V, the $\Delta i_p^{EP}/\Delta i_p^{UA}$ was even closer to 1 compared to an amplitude of 0.010 V (Fig. S4b). However, the peaks corresponding to EP and UA were poorly defined (Fig. S4c). Consequently, an optimal amplitude of 0.010 V was chosen for the next optimization procedure.

The frequency was varied from 10 Hz to 25 Hz, with an increment of 1 Hz (Fig. S5c). The widest $\left|E_p^{EP} - E_p^{UA}\right|$ and the $\Delta i_p^{EP}/\Delta i_p^{UA}$ closest to 1 were both observed at a frequency of 10 Hz (Fig. S5a,b). Therefore, a frequency of 10 Hz was selected as the optimal frequency for the next optimization procedure.

The E_{step} was varied in a range from 0.001 V to 0.010 V, with an increment of 0.001 V (Fig. S6c). The widest $\left|E_p^{EP} - E_p^{UA}\right|$ was observed at an E_{step} of 0.010 V (Fig. S6a). The $\Delta i_p^{EP}/\Delta i_p^{UA}$ closest to 1 was determined at an E_{step} of 0.009 and 0.010 V (Fig. S6b). Since an E_{step} of 0.010 V showed the widest $\left|E_p^{EP} - E_p^{UA}\right|$, it was chosen as the optimal E_{step} for for the next optimization procedure.

3.4. The effect of changing pH on the electroanalytical performance of the pLC-SPCE sensor

The optimization of the pH of 0.1 M PBS solution to obtain the best electroanalytical performance of the pLC-SPCE sensor was performed. The pH at which the widest $\left|E_p^{EP} - E_p^{UA}\right|$, the $\Delta i_p^{EP}/\Delta i_p^{UA}$ closest to 1, the highest Δi_p^{EP}, and the highest Δi_p^{UA} were obtained was considered to be the optimal pH. In order to optimize the pH, solutions of 0.1 M PBS containing 1.0 mg/L of EP and UA were prepared with pH values ranging from 2.00 to 10.00, with an increment of 1.00. Six measurements were performed at each pH value tested.

The widest $\left|E_p^{EP} - E_p^{UA}\right|$ was observed at a pH of 10.00 (Fig. S7c). However, at this pH, the Δi_p^{EP} and Δi_p^{UA} were among the lowest compared to the measurements at other pH values (Figs. S7a,b). Moreover, the $\Delta i_p^{EP}/\Delta i_p^{UA}$ was close to zero as the peak for EP was barely formed (Fig. S7d).

The highest Δi_p^{EP} and Δi_p^{UA} were observed at pH values of 5.00 and 4.00, respectively (Figs. S7a,b). At a pH of 5.00, the $\Delta i_p^{EP}/\Delta i_p^{UA}$ was closer to 1 than for the measurements at a pH of 4.00 (Fig. S7d). On the other hand, at a pH of 4.00, a wider $\left|E_p^{EP} - E_p^{UA}\right|$ was achieved compared to a pH of 5.00 (Fig. S7c). Therefore, an additional experiment was performed at a pH of 4.50. The highest Δi_p for both analytes was obtained at this pH (Figs. S7a,b). In addition, the $\Delta i_p^{EP}/\Delta i_p^{UA}$ was close to 1 (the closest of all pH values tested, Fig. S7d). Therefore, a pH of 4.50 was selected as the optimal pH for for the next optimization procedure.

A linear relationship was obtained between the E_p^{EP} and E_p^{UA} vs. pH in a range from 2.00 to 10.00 with the regression equations of $E_p^{EP} = -$

$63.8 \cdot pH + 432.7$ (Fig. S7e) and $E_p^{UA} = -61.6 \cdot pH + 557.9$(Fig. S7f), respectively. The slopes for EP and UA were –63.8 mV/pH and –61.6 mV/pH, respectively, which was close to the theoretical value of 59.2 mV/pH, if the number of exchanged protons and electrons is equal [40]. This was consistent with the reaction mechanism for both analytes [41].

3.5. The effect of changing E_{dep} and t_{dep} on the electroanalytical performance of the pLC-SPCE sensor

The E_{dep} and t_{dep} were optimized to obtain the best electroanalytical performance of the pLC–SPCE sensor. All measurements were performed in triplicate in 0.1 M PBS (pH = 4.50) containing 1.0 mg/L of EP and UA. SWAdSV measurements were performed in an E range from −0.100 V to 0.400 V. The E_{dep} and t_{dep} at which the highest Δi_p^{EP} and Δi_p^{UA} were obtained were considered to be the optimal E_{dep} and t_{dep}. In addition, the E_{dep} and t_{dep} that produce the widest $\left|E_p^{EP} - E_p^{UA}\right|$ and the $\Delta i_p^{EP}/\Delta i_p^{UA}$ closest to 1 were also considered.

The E_{dep} was varied from 0.000 V to −0.800 V. In general, applying a more negative E_{dep} resulted in an increased oxidation peak for EP and a decreased oxidation peak for UA (Figs. S8a,b,e). Fig. S8e shows that for SWAdS voltammograms, the E_{dep} only affects the oxidation peak for EP, while it did not have a significant effect on the oxidation peak of UA. The decrease in the oxidation peak of UA can be attributed to the increase in the oxidation peak of EP. This is consistent with the ToF-SIMS measurements by which UA was not detected on the surface of the pLC-SPCE after applying E_{dep}, whereas EP was present. This is another indicator of why the $\Delta i_p^{EP}/\Delta i_p^{UA}$ should be close to 1. The highest Δi_p^{EP} and Δi_p^{UA} were observed at an E_{dep} of −0.600 V and 0.000 V, respectively (Figs. S8a,b). Since the highest Δi_p for both analytes was observed at different E_{dep}, additional evaluation of these two E_{dep} in terms of $\left|E_p^{EP} - E_p^{UA}\right|$ and the $\Delta i_p^{EP}/\Delta i_p^{UA}$ was performed. The $\Delta i_p^{EP}/\Delta i_p^{UA}$ closest to 1 was observed at an E_{dep} of 0.000 V as compared to −0.600 V (Fig. S8d). Moreover, a wider $\left|E_p^{EP} - E_p^{UA}\right|$ was also obtained at an E_{dep} of 0.000 V than at −0.600 V (Fig. S8c). Thus, an E_{dep} of 0.000 V was selected as the optimal E_{dep} for the next optimization procedure.

The effect of different t_{dep} was studied in a range from 0 s to 120 s (Figs. S9a–e). The highest Δi_p^{EP} was obtained at 15 s (Fig. S9a), while the highest Δi_p^{UA} was obtained at 30 s (Fig. S9b). After 15 s and 30 s for EP and UA, respectively, the Δi_p^{EP} and Δi_p^{UA} started to decrease slightly with increasing t_{dep}. The decrease in Δi_p^{EP} and Δi_p^{UA} is most likely a consequence of the saturation of EP and UA on the pLC–SPCE surface, limiting the available active sites for further oxidation of both analytes, leading to an observed decrease in the Δi_p^{EP} and Δi_p^{UA} [42,43]. The $\left|E_p^{EP} - E_p^{UA}\right|$ were similar for a t_{dep} of 15 s and 30 s (Fig. S9c). Of all t_{dep} tested, the $\Delta i_p^{EP}/\Delta i_p^{UA}$ closest to 1 was obtained for a t_{dep} of 15 s (Fig. S9d). Therefore, 15 s was selected as the optimal t_{dep} for the analysis.

Next, method validation was performed using the optimized parameters in Sections 3.2–3.5 for EP and UA. The LOD, limit of quantification (LOQ), linear concentration range, accuracy, and precision were determined. Additionally, an interference effect study and real sample analysis were performed.

3.6. The limits of detection and limits of quantification

The LOD and LOQ were determined experimentally based on the signal-to-noise ratio (S/N), which had to be greater than or equal to 3.00 for LOD and greater than or equal to 10.00 (but close to 10.00) for LOQ [44]. Three replicates were performed, each with a new pLC-SPCE sensor. The values for the LOD and LOQ for both analytes were reported as the highest LODs and LOQs from three replicates. The determined LODs for both analytes were 10.0 μg/L at an S/N of 5.93 for EP and 6.35 for UA. The determined LOQs for both analytes were 19.8 μg/L at an S/N of 14.24 and 11.00 for EP and UA, respectively. The SWAdS voltammograms for LOD and LOQ determination are shown in Fig. S10. As this is, to the best of our knowledge, the first reported simultaneous analysis of EP and UA on a modified SPCE (the pLC–SPCE in this work), a comparison between the pLC-SPCE and other modified (conventional) electrodes was performed (Table 1). The determined LODs and LOQs for EP and UA were among the lowest values reported previously (Table 1).

3.7. Linear concentration ranges

The successive additions of solutions of EP and UA standards were pipetted in an electrochemical cell to determine the ranges in which the Δi_p^{EP} and Δi_p^{UA} change linearly with their mass concentrations (γ). After each addition, the SWAdS voltammogram was measured and the resulting Δi_p^{EP} and Δi_p^{UA} were plotted vs. the γ of EP and UA, respectively. The method was deemed to be linear if the square of the correlation coefficient (R^2) was greater than or equal to 0.9900 for both analytes. The linear concentration range for EP and UA was determined three times using a different pLC-SPCE sensor for each determination.

Two linear concentration ranges were determined for EP and UA. The first linear concentration range was from 49.0 μg/L to 326.1 μg/L (Fig. 4), while the second linear concentration range was from 326.1 μg/L to 887.1 μg/L (Fig. 4) for both analytes. The R^2 was greater than 0.9900 for both analytes for all three replicates (Fig. 4).

3.8. Accuracy and precision

The accuracy and precision were determined at the low and middle concentration levels of the two linear concentration ranges for both analytes. The prepared concentrations, i.e. the theoretical mass concentrations ($\gamma_{theoretical}$), of both analytes tested at the low and middle concentration levels of the first linear concentration range (from 49.0 μg/L to 326.1 μg/L) were 50.2 μg/L and 190.1 μg/L, respectively. For the second linear concentration range (from 326.1 μg/L to 887.1 μg/L), the $\gamma_{theoretical}$ of both analytes tested at the low and middle concentrations levels were 330.8 μg/L and 660.3 μg/L, respectively. Six replicates were measured for each concentration level tested. The accuracy and precision were evaluated based on the recovery (Re) and relative standard deviation (RSD), respectively. The method was deemed to be accurate when the average Re was in a range from 80.0% to 120.0%, and precise when the RSD was less than or equal to 20.0% [53]. The quantification was performed by employing the calibration curve. The accuracy and precision results for both analytes are shown in Table 2.

The average Re for all concentration levels tested was within a range from 80.0% to 120.0% for both analytes (Table 2). The low concentration level tested (i.e. 50.2 μg/L) of the first linear concentration range had the largest deviation from the Re of 100.0% for both analytes, with an average Re of 108.4% for EP and 94.4% for UA (Table 2). The average Re values at the other concentration levels tested were closer to 100.0%, ranging from 97.2% to 98.0% for EP and from 97.8% to 99.8% for UA (Table 2).

The RSD values for both analytes were considerably less than 20.0% (Table 2). The low concentration level tested of the first linear concentration range resulted in the largest RSD values, which were 11.7% for EP and 10.7% for UA. The RSD values for the other tested concentration levels ranged from 2.6% to 3.1% for EP and from 4.1% to 5.7% for UA (Table 2).

Based on these results, the method for the simultaneous determination of EP and UA using the pLC–SPCE sensor was deemed to be accurate and precise.

3.9. Interference effect study

The interference effect was investigated to determine whether the

Table 1
A comparison of electrochemical techniques, linear concentration ranges, LODs, and real sample analyses for the simultaneous determination of EP and UA determined with various modified electrodes.

Electrode	Technique	Linear concentration ranges / (mol/L)	LOD / (mol/L)	Real sample application	Reference
CuTe/GP[a]	DPV[b]	$5 \cdot 10^{-6}$ – $60 \cdot 10^{-6}$ for EP $5 \cdot 10^{-6}$ – $120 \cdot 10^{-6}$ for UA	$18 \cdot 10^{-9}$ for EP $32 \cdot 10^{-9}$ for UA	Pharmaceutical and clinical samples	[45]
Poly(caffeic acid)/GCE	CV	$2.0 \cdot 10^{-6}$ – $8.0 \cdot 10^{-5}$ for EP $5.0 \cdot 10^{-6}$ – $3.0 \cdot 10^{-4}$ for UA	$200 \cdot 10^{-9}$ for EP $600 \cdot 10^{-9}$ for UA	EP hydrochloride injection and mixed sample	[46]
OMC/Nafion/GCE[c]	DPV	$0.5 \cdot 10^{-6}$ – $200 \cdot 10^{-6}$ for EP $0.25 \cdot 10^{-6}$ – $100 \cdot 10^{-6}$ for UA	$200 \cdot 10^{-9}$ for EP $70 \cdot 10^{-9}$ for UA	EP hydrochloride injection and human urine	[47]
Electrochemically activated GCE	DPV	$1.0 \cdot 10^{-6}$ – $4.0 \cdot 10^{-5}$ for EP $1.0 \cdot 10^{-6}$ – $5.5 \cdot 10^{-5}$ for UA	$89 \cdot 10^{-9}$ for EP $160 \cdot 10^{-9}$ for UA	EP hydrochloride injection and serum	[48]
sG/Pd/GCE[d]	DPV	$2.0 \cdot 10^{-6}$ – $50.0 \cdot 10^{-6}$ for EP $10.0 \cdot 10^{-6}$ – $100 \cdot 10^{-6}$ for UA	$100 \cdot 10^{-9}$ for EP $170 \cdot 10^{-9}$ for UA	Blood serum and urine	[49]
Au/ZnO/PPy/RGO/GCE[e]	DPV	$0.6 \cdot 10^{-6}$ – $500 \cdot 10^{-6}$ for EP $1.0 \cdot 10^{-6}$ – $680 \cdot 10^{-6}$ for UA	$60 \cdot 10^{-9}$ for EP $90 \cdot 10^{-9}$ for UA	Synthesis samples, pharmaceutical samples, urine	[33]
PXSP/GCE[f]	DPV	$2 \cdot 10^{-6}$ – $390 \cdot 10^{-6}$ for EP $0.1 \cdot 10^{-6}$ – $560 \cdot 10^{-6}$ for UA	$100 \cdot 10^{-9}$ for EP $80 \cdot 10^{-9}$ for UA	Pharmaceutical and urine samples	[50]
Poly(DA)-nanogold/GCE[g]	CV, SWV	$1.0 \cdot 10^{-6}$ – $80.0 \cdot 10^{-6}$ for EP $0.8 \cdot 10^{-6}$ – $100.0 \cdot 10^{-6}$ for UA	$100 \cdot 10^{-9}$ for EP $60 \cdot 10^{-9}$ for UA	Human serum and urine	[51]
PEBT/ERGO/GCE[h]	DPV	$8.0 \cdot 10^{-7}$ – $7.0 \cdot 10^{-5}$ for EP $5.0 \cdot 10^{-6}$ – $1.4 \cdot 10^{-4}$ for UA	$400 \cdot 10^{-9}$ for EP $1000 \cdot 10^{-9}$ for UA	Blood sera serum	[52]
pLC-SPCE	SWAdSV	$0.27 \cdot 10^{-6}$ – $1.78 \cdot 10^{-6}$ and $1.78 \cdot 10^{-6}$ – $4.84 \cdot 10^{-6}$ for EP and UA	$54.6 \cdot 10^{-9}$ (10.0 μg/L) for EP and UA	Auto-injector and human urine	This work

[a] CuTe/GP (copper telluride modified graphite paste electrode)
[b] DPV (differential pulse voltammetry)
[c] OMC/Nafion/GCE (ordered mesoporous carbon nafion modified GCE)
[d] sG/Pd/GCE (reduced graphene oxide palladium modified GCE)
[e] Au/ZnO/PPy/RGO/GCE (reduced graphene oxide(RGO)/polypyrrole(PPy)/zinc oxide(ZnO)/gold(Au) nanoparticles nanocomposite modified GCE
[f] PXSP/GCE (poly(p–xylenolsulfonephthalein) modified GCE)
[g] poly(DA)-nanogold/GCE (polydopamine (PDA)-nanogold composites modified GCE)
[h] PEBT/ERGO/GCE (polymer of erichrome black T (PEBT)/electrochemically reduced graphene oxide (ERGO)/GCE)

presence of several different compounds (potential interferents) had a significant effect on the Δi_p^{EP} and Δi_p^{UA}. The interferents were selected based on their occurrence in real samples, such as an EP auto-injector and human urine. The interferents tested were glucose, L-AA, K^+, Cl^-, Ca^{2+}, SO_4^{2-}, Mg^{2+}, NH_4^+, $C_2O_4^{2-}$, and urea.

The effect of potential interferents on the Δi_p^{EP} and Δi_p^{UA} was evaluated using the relative error (E_{rel}) as E_{rel} (%) $= \left|\frac{\Delta i_p^{interferent} - \Delta i_p^{analyte}}{\Delta i_p^{analyte}}\right| \cdot 100$, where $\Delta i_p^{interferent}$ is the Δi_p^{EP} or Δi_p^{UA} measured in 0.1 M PBS (pH = 4.50) containing 500.0 μg/L of EP and UA and 500.0 μg/L of possible interferent, and $\Delta i_p^{analyte}$ is the Δi_p^{EP} or Δi_p^{UA} measured in 0.1 M PBS (pH = 4.50) containing 500.0 μg/L of EP and UA, without the presence of interferent. The γ ratio between the analytes (EP and UA) and interferent was 1:1, as the γ of both analytes and interferent was 500.0 μg/L. Three replicates were performed, and the average E_{rel} ($\overline{E_{rel}}$) was calculated. The interference effect was considered significant when the $\overline{E_{rel}}$ was higher than 10.00%. The results are shown in Fig. 5, and the corresponding SWAdS voltammograms for one replicate are shown in Fig. S11.

The $\overline{E_{rel}}$ for all tested potential interferents were less than 10.00% for both analytes (Fig. 5). Among these compounds, the highest $\overline{E_{rel}}$ for EP was observed in the presence of L-AA with an $\overline{E_{rel}}$ of 7.39%, while the $\overline{E_{rel}}$ for other compounds were in a range from 0.78% to 2.13% (Fig. 5a,c). For UA, the highest $\overline{E_{rel}}$ occurred in the presence of Mg^{2+} ions with an $\overline{E_{rel}}$ of 4.33% (Fig. 5b,c). The $\overline{E_{rel}}$ for other compounds were in a range from 1.52% to 3.82% (Fig. 5b,c). In the presence of K^+, Ca^{2+}, Mg^{2+}, and NH_4^+, the E_p^{EP} and E_p^{UA} slightly shifted toward a more positive E (Figs. S11c,e,g, h). Additionally, the baseline of the SWAdSV measurement slightly increased in the presence of these cations. However, despite these changes, they did not have a significant effect on the Δi_p^{EP} or Δi_p^{UA}. Therefore, it can be concluded that none of the tested compounds had a significant interference effect on the Δi_p^{EP} or Δi_p^{UA}.

3.10. Analysis of EP in an auto-injector and UA in human urine

The applicability of the validated method for the simultaneous determination of EP and UA using the pLC-SPCE sensor was tested for a real sample, i.e. EP auto-injector and UA in human urine samples. The content of EP in EP auto-injector and UA in human urine samples was determined. To test the accuracy and precision of the method for real sample analysis, the EP auto-injector and human urine were spiked with a known amount of solution of EP or UA standard, respectively. The same criteria for accuracy and precision were considered for the real samples, as given in Section 3.8. The quantification was carried out using a calibration curve. Four different urine samples were collected from healthy individuals and analysed on the same day without any sample pretreatment. One individual (sample 1) was instructed to consume a large amount of water to become highly hydrated. This was done to test whether the UA concentration in this urine sample would be below the lower limit of the normal range of UA in human urine. According to the literature, the normal range of UA concentration in human urine for a healthy individual is between 235.5 mg/L and 738.7 mg/L [9]. Three replicates were performed for every human urine sample tested, and the results are shown in Table 3.

The SWAdS voltammograms for UA determination in the real sample are shown in Fig. S12 (the first of the replicates), where no oxidation peak for EP was detected for any of the four analysed samples (Fig. S12). On the other hand, well–defined oxidation peaks for UA were observed. This indicates that EP was not present in the human urine or the concentration of EP in the human urine was below the method's LOD.

The $\overline{\gamma}_{sample}$ of the four analysed samples ranged from 123.4 mg/L to 582.7 mg/L (Table 3). The $\overline{\gamma}_{sample}$ of samples 2–4 was within the normal range, whereas the $\overline{\gamma}_{sample}$ of sample 1 was below the normal range. This may be attributed to the extreme hydration of the individual from whom sample 1 was collected. The results of all four samples were deemed to be accurate and precise as the average Re was within 80.0–120.0%, and the RSD values were well below 20.0%, respectively.

The EP auto-injector, with a declared concentration of 150 μg/0.3

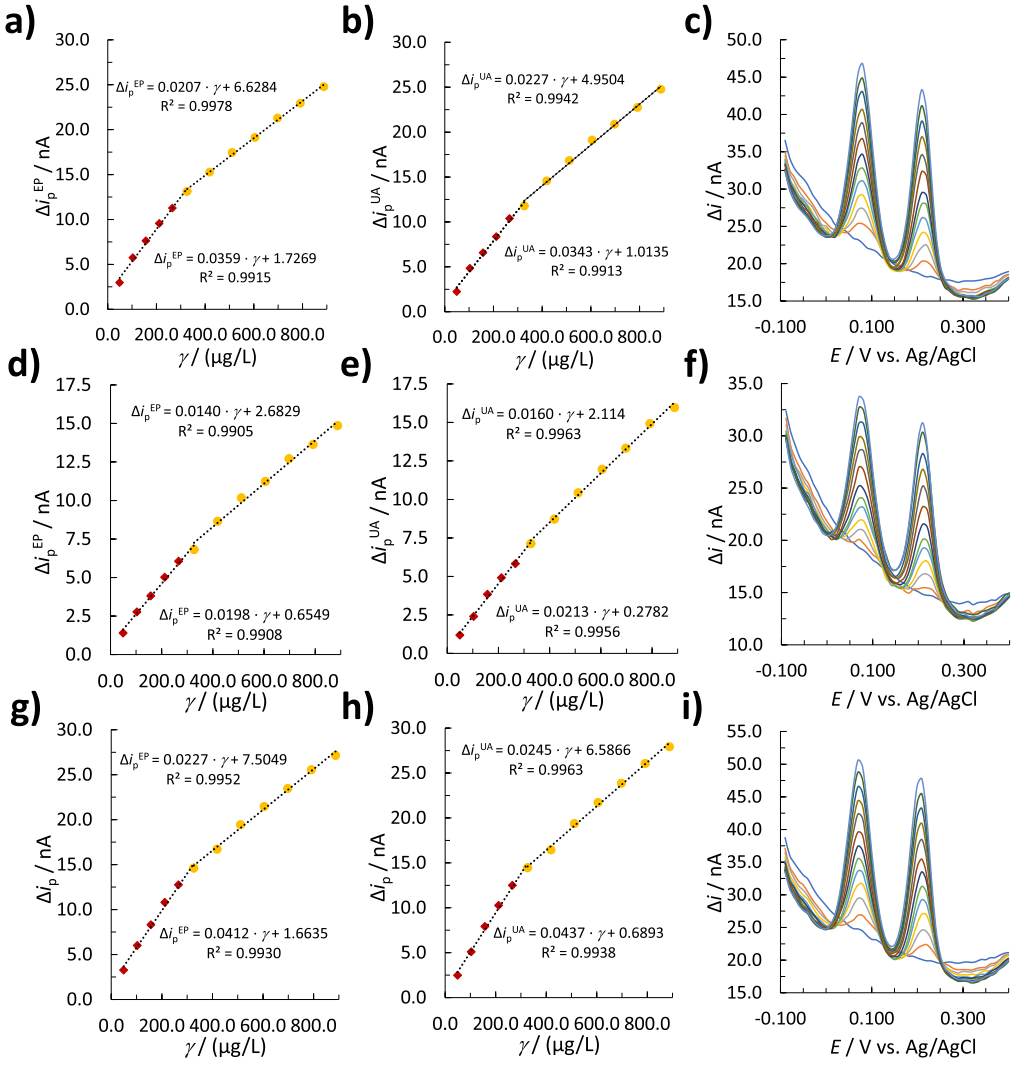

Fig. 4. a–c) The 1st replicate, d–f) the 2nd replicate, and g–i) the 3rd replicate of the linear concentration range determination. a,d,g) The obtained linear concentration ranges for EP, b,e,h) the obtained linear concentration ranges for UA, and c,f,i) the SWAdS voltammograms measured in 0.1 M PBS (pH = 4.50) containing the solutions of EP and UA standards with γ ranging from 49.0 µg/L to 887.1 µg/L.

Table 2
The accuracy and precision results measured at the low and middle concentration levels of the two linear concentration ranges for both analytes, where the $\overline{\gamma}_{determined}$ is the measured γ.

Analyte	$\gamma_{theoretical}$ / (µg/L) ($n = 6$)	$\overline{\gamma}_{determined}$ / (µg/L) ($n = 6$)	Average Re / % ($n = 6$)	RSD / %
EP	50.2	54.4	108.4	11.7
	190.1	185.3	97.5	3.1
	330.8	321.6	97.2	3.1
	660.3	588.5	98.0	2.6
UA	50.2	47.4	94.4	10.7
	190.1	185.9	97.8	4.9
	330.8	324.7	98.1	4.1
	660.3	598.9	99.8	5.7

mL (corresponding to 500.0 mg/L), was analysed six times without sample pretreatment, and the results are shown in Table 4. The corresponding SWAdS voltammograms are shown in Fig. S13.

The determined $\overline{\gamma}_{sample}$ of the EP auto-injector was 491.5 mg/L. The accuracy and precision of the obtained results were also confirmed as the average Re (102.2%) was within the range 80.0–120.0%, and the RSD was well below 20.0%.

4. Conclusions

A simple, selective, and cost-effective sensor based on a poly(L-cysteine) film modified screen–printed carbon electrode (pLC-SPCE) sensor was developed for the simultaneous determination of epinephrine (EP) and uric acid (UA) using a square-wave adsorptive stripping voltammetry (SWAdSV) method. The surface modification of the SPCE sensor was made by the electropolymerization of L–cysteine (LC) using multiple cyclic voltammetry sweeps, resulting in the formation of pLC film. The successful formation of this film was proved by time-of-flight secondary ion mass spectrometry, i.e. the presence of LC and its electropolymerization product (L-cysteic acid) was confirmed. The electroactivation of the pLC-SPCE sensor was necessary to obtain a steady baseline for subsequent SWAdSV measurements in 0.1 M PBS (pH = 4.50). This was achieved by performing 10 consecutive square-wave voltammetry sweeps in 0.1 M PBS (pH = 4.50). A comparison of the bare SPCE and the pLC-SPCE showed that the presence of pLC film on the surface of the SPCE sensor improves peak–to–peak separation and increases the signal for EP and UA. The optimization of amplitude, frequency, potential step (E_{step}), the pH of 0.1 M PBS solution, the concentration of LC and number of cycles during electropolymerization, the deposition potential (E_{dep}), and the deposition time (t_{dep}) was

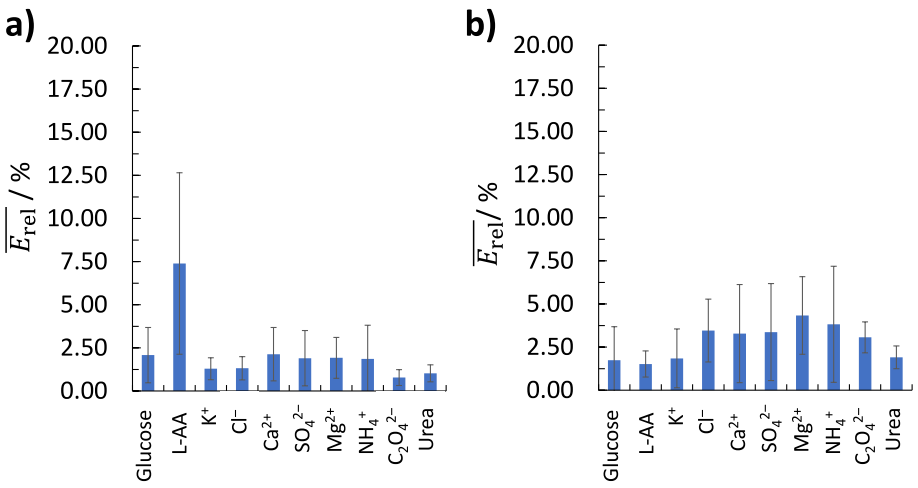

Fig. 5. The plot of $\overline{E_{rel}}$ values vs. different interferents for a) EP and b) UA. The error bars represent the standard deviations.

Table 3
The results of UA determination for human urine analysis for four different samples.

Sample	[a] $\overline{\gamma}_{\text{initially determined}}$ / (μg/L) (n = 3)	[b] $\overline{\gamma}_{\text{spiked}}$ / (μg/L) (n = 3)	Average Re / % (n = 3)	RSD / %	[c] $\overline{\gamma}_{\text{sample}}$ in human urine (mg/L) (n = 3)
1	123.4	199.9	102.6	1.7	123.4
2	393.9	493.8	96.4	4.1	393.9
3	525.5	626.6	102.5	8.7	525.5
4	582.7	681.1	102.5	8.0	582.7

[a] The determined γ of the diluted real sample.
[b] The determined γ after spiking the real sample with a solution of a known amount of EP or UA standard.
[c] The calculated analyte's γ in the real sample by taking into account the dilution factor.

Table 4
The results of the EP auto-injector analysis. Six replicates were performed.

Replicate	$\overline{\gamma}_{\text{determined}}$ / (μg/L)	$\overline{\gamma}_{\text{spiked}}$ / (μg/L)	Re / %	RSD / %	$\overline{\gamma}_{\text{sample}}$ in auto-injector / (mg/L) (n = 6)
1st	482.3	586.7	103.8	4.9	491.5
2nd	529.9	641.3	111.4		
3rd	486.9	584.1	98.2		
4th	471.1	570.5	99.3		
5th	475.4	573.4	98.5		
6th	503.4	604.8	102.2		

performed. The optimal amplitude, frequency, and E_{step} were determined to be 0.010 V, 10 Hz, and 0.010 V, respectively. The optimal pH of the 0.1 M PBS solution was 4.50. For electropolymerization, an optimal LC concentration of 2 mM and 10 cycle sweeps using cyclic voltammetry were determined. Finally, the optimal E_{dep} and t_{dep} were determined to be 0.000 V and 15 s, respectively.

Next, using these optimized parameters, the method was validated. The LODs and LOQs for both analytes were determined to be 10.0 μg/L and 19.8 μg/L, respectively. Two linear concentration ranges were obtained for EP and UA. For both analytes, the first linear concentration range was between 49.0 μg/L and 326.1 μg/L, while the second linear concentration range was between 326.1 μg/L and 887.1 μg/L. The average recoveries (Re) and relative standard deviations (RSDs) at the low and middle concentration levels of the first linear concentration range were in a range from 94.4% to 108.4% (n = 6) and from 3.1 to 10.7% (n = 6), respectively, for both analytes. For the second linear concentration range, the average Re and RSDs at the low and middle concentration levels for both analytes were in a range from 97.2% to 99.8% (n = 6) and from 2.6% to 5.7% (n = 6), respectively. The latter proves that the method produces accurate and precise results. Moreover, the interference study showed that glucose, L-AA, K^+, Cl^-, Ca^{2+}, SO_4^{2-}, Mg^{2+}, NH_4^+, $C_2O_4^{2-}$, and urea had no significant effect on the EP and UA signals. Moreover, the method was successfully employed to analyse four different human urine samples, showing the high accuracy and precision of the results with the average Re and RSDs in a range from 96.4% to 102.6% and from 1.7 to 8.7%, respectively. Furthermore, the developed method also demonstrated accurate and precise results for the determination of EP in an auto-injector, with an average Re of 102.2% and RSD of 4.9%.

The small, portable, selective, and cost-effective design of the pLC-SPCE sensor, along with its improved peak-to-peak separation and enhanced signal for EP and UA, make it a highly advantageous choice over conventional methods for the simultaneous determination of UA and EP in real samples without sample pretreatment.

CRediT authorship contribution statement

David Majer: Conceptualization, Methodology, Software, Visualization, Writing – original draft, Writing – review & editing. **Matjaž Finšgar:** Funding acquisition, Methodology, Project administration, Resources, Supervision, Visualization, Writing – review & editing.

Declaration of Competing Interest

The authors declare that they have no known competing financial interests or personal relationships that could have appeared to influence the work reported in this paper.

Data availability

Data will be made available on request.

Acknowledgments

The authors acknowledge the financial support of the Slovenian Research Agency (Grant Numbers: P2-0414, P2-0118, and J1-4416).

Appendix A. Supplementary data

Supplementary data to this article can be found online at https://doi.

org/10.1016/j.microc.2023.109142.

References

[1] D.S. Sipuka, T.I. Sebokolodi, F.O.G. Olorundare, C. Muzenda, O.V. Nkwachukwu, D. Nkosi, O.A. Arotiba, Electrochemical sensing of epinephrine on a carbon nanofibers and gold nanoparticle-modified electrode, Electrocatalysis 14 (2023) 9–17.

[2] I.A. Mattioli, P. Cervini, É.T.G. Cavalheiro, Screen-printed disposable electrodes using graphite-polyurethane composites modified with magnetite and chitosan-coated magnetite nanoparticles for voltammetric epinephrine sensing: a comparative study, Microchim. Acta 187 (2020) 318.

[3] X. Yang, P. Zhao, Z. Xie, M. Ni, C. Wang, P. Yang, Y. Xie, J. Fei, Selective determination of epinephrine using electrochemical sensor based on ordered mesoporous carbon / nickel oxide nanocomposite, Talanta 233 (2021), 122545.

[4] A. Muraro, M. Worm, C. Alviani, V. Cardona, A. DunnGalvin, L.H. Garvey, C. Riggioni, D. de Silva, E. Angier, S. Arasi, A. Bellou, K. Beyer, D. Bijlhout, M.B. Bilò, C. Bindslev-Jensen, K. Brockow, M. Fernandez-Rivas, S. Halken, B. Jensen, E. Khaleva, L.J. Michaelis, H.N.G. Oude Elberink, L. Regent, A. Sanchez, B.J. Vlieg-Boerstra, G. Roberts, E.A.o. Allergy, F.A. Clinical Immunology, Anaphylaxis Guidelines Group, EAACI guidelines: Anaphylaxis (2021 update), Allergy, 77 (2022) 357-377.

[5] T.E. Dribin, S. Waserman, P.J. Turner, Who needs epinephrine? Anaphylaxis, autoinjectors, and parachutes, The Journal of Allergy and Clinical Immunology In Pract. 11 (2023) 1036–1046.

[6] S. Dreborg, G. Walter, H. Kim, International recommendations on epinephrine auto-injector doses often differ from standard weight-based guidance: a review and clinical proposals, Allergy Asthma Clin. Immunol. 18 (2022) 102.

[7] H.V.M. Hai, D.Q. Khieu, T.K. Vo, V.C. Nguyen, J. Kim, Synthesis of ternary core-shell carbon sphere@α-Fe2O3@Ag composites and their application for simultaneous voltammetric detection of uric acid, xanthine, and hypoxanthine, Korean J. Chem. Eng. 40 (2023) 657–666.

[8] M. Ahsan, T.F. Manny, M.M. Hossain, M.R. Miah, M.A. Aziz, M.A. Hasnat, Spontaneous immobilization of thiocyanate onto Au surface for the detection of uric acid in basic medium, Surf. Interfaces 36 (2023), 102599.

[9] F. Li, T. He, S. Wu, Z. Peng, P. Qiu, X. Tang, Visual and colorimetric detection of uric acid in human serum and urine using chitosan stabilized gold nanoparticles, Microchem. J. 164 (2021), 105987.

[10] O. Gyllenhaal, L. Johansson, J. Vessman, Gas chromatography of epinephrine and norepinephrine after derivatization with chloroformates in aqueous media, J. Chromatogr. A 190 (1980) 347–357.

[11] Y.-P. Sun, J. Chen, H.-Y. Qi, Y.-P. Shi, Graphitic carbon nitrides modified hollow fiber solid phase microextraction for extraction and determination of uric acid in urine and serum coupled with gas chromatography-mass spectrometry, J. Chromatogr. B 1004 (2015) 53–59.

[12] A.M. Cohen, L. Wiseman, A. Al Faraj, P. Andreou, R. Hall, V.M. Neira, Use of a liquid chromatography-tandem mass spectrometry method to assess the concentration of epinephrine, norepinephrine, and phenylephrine stored in plastic syringes, 8 (2023).

[13] M. Kopčil, R. Kaňďár, Screening method for the simultaneous determination of allantoin and uric acid from dried blood spots, J. Pharm. Biomed. Anal. 225 (2023), 115222.

[14] N.N. A'in, A. Ulianas, N. Azwir, I.G. Fauzi, Wahyudi, Uric acid analysis using AgNO3 with UV-Vis spectrophotometry method, AIP Conference Proceedings, 2673 (2023).

[15] M.Q. Al Abachi, H. Hadi, A new kinetic and thermodynamic study of spectrophotometric method for determination of adrenaline in its pharmaceutical formulations, Pharm. Chem. J. 48 (2014) 558–563.

[16] T. Li, Z. Wang, H. Xie, Z. Fu, Highly sensitive trivalent copper chelate-luminol chemiluminescence system for capillary electrophoresis detection of epinephrine in the urine of smoker, J. Chromatogr. B 911 (2012) 1–5.

[17] J.C. Fanguy, C.S. Henry, The analysis of uric acid in urine using microchip capillary electrophoresis with electrochemical detection, Electrophoresis 23 (2002) 767–773.

[18] D. Majer, M. Finšgar, An l-cysteic acid-modified screen-printed carbon electrode for methyl parathion determination, Microchem. J. 183 (2022), 108098.

[19] M. Sayed Zia, F. Mosazadeh, H. Beitollah, Z. Barani, A novel electrochemical sensor for epinephrine in the presence of acetylcholine based on modified screen-printed electrode, Russ. J. Electrochem. 58 (2022) 248–257.

[20] M. Sisay, A. Kassa, A. Tesfaye, Highly selective square wave voltammetric determination of gallic acid in groundnut and tea samples using glycine(2-aminoethanoic acid) modified carbon paste electrode, Sensors International 4 (2023), 100227.

[21] V. Mirceski, R. Gulaboski, M. Lovric, I. Bogeski, R. Kappl, M. Hoth, Square-wave voltammetry: a review on the recent progress, Electroanalysis 25 (2013) 2411–2422.

[22] S.C. Wang, K.S. Chang, C.J. Yuan, Enhancement of electrochemical properties of screen-printed carbon electrodes by oxygen plasma treatment, Electrochim. Acta 54 (2009) 4937–4943.

[23] A. Mahanta, U.S. Akond, K. Barman, S. Jasimuddin, Electrochemical sensing of dopamine and epinephrine using self-assembled Fe3O4 magnetic nanoparticles on a pyridine-grafted glassy carbon electrode, Electroanalysis 34 (2022) 1780–1788.

[24] S. Kalia, D.S. Rana, N. Thakur, D. Singh, R. Kumar, R.K. Singh, Two-dimensional layered molybdenum disulfide (MoS2)-reduced graphene oxide (rGO) heterostructures modified with Fe3O4 for electrochemical sensing of epinephrine, Mater. Chem. Phys. 287 (2022), 126274.

[25] B. Wu, S. Yeasmin, Y. Liu, L.-J. Cheng, Sensitive and selective electrochemical sensor for serotonin detection based on ferrocene-gold nanoparticles decorated multiwall carbon nanotubes, Sens. Actuators B 354 (2022), 131216.

[26] A. Hashem, A.R. Marlinda, M.A.M. Hossain, M. Al Mamun, M. Shalauddin, K. Simarani, M.R. Johan, A unique oligonucleotide probe hybrid on graphene decorated gold nanoparticles modified screen-printed carbon electrode for pork meat adulteration, Electrocatalysis 14 (2023) 179–194.

[27] J. Lerdsri, J. Upan, J. Jakmunee, Nafion mixed carbon nanotube modified screen-printed carbon electrode as a disposable electrochemical sensor for quantification of Amitraz in honey and longan samples, Electrochim. Acta 410 (2022), 140050.

[28] J.G. Manjunatha, M. Deraman, N.H. Basri, I.A. Talib, Fabrication of poly (Solid Red A) modified carbon nano tube paste electrode and its application for simultaneous determination of epinephrine, uric acid and ascorbic acid, Arab. J. Chem. 11 (2018) 149–158.

[29] W. Khamcharoen, C.S. Henry, W. Siangproh, A novel l-cysteine sensor using in-situ electropolymerization of l-cysteine: potential to simple and selective detection, Talanta 237 (2022), 122983.

[30] X. Cui, Z. Luo, M. Guo, J. Xu, L. Wang, G. Chen, G. Wang, C. Chang, A. Zeng, J. Zhang, Q. Fu, A new multi-identification system based on a poly(l-cysteine) sensor for simultaneous detection of multiple steroid hormones in serum, Chem. Eng. J. 455 (2023), 140812.

[31] G.S. Ustabasi, C. Pérez-Ràfols, N. Serrano, J.M. Díaz-Cruz, Simultaneous determination of iron and copper using screen-printed carbon electrodes by adsorptive stripping voltammetry with o-phenanthroline, Microchem. J. 179 (2022), 107597.

[32] P. Kalimuthu, S.A. John, Simultaneous determination of epinephrine, uric acid and xanthine in the presence of ascorbic acid using an ultrathin polymer film of 5-amino-1,3,4-thiadiazole-2-thiol modified electrode, Anal. Chim. Acta 647 (2009) 97–103.

[33] K. Ghanbari, A. Hajian, Electrochemical characterization of Au/ZnO/PPy/RGO nanocomposite and its application for simultaneous determination of ascorbic acid, epinephrine, and uric acid, J. Electroanal. Chem. 801 (2017) 466–479.

[34] B. Regis, L. Ferraz, F. Roberto, F. Leite, A.R. Malagutti, Simultaneous determination of ethionamide and pyrazinamide using poly(l-cysteine) film-modified glassy carbon electrode, Talanta 154 (2016) 197–207.

[35] W. Wang, Z. Yi, Q. Liang, J. Zhen, R. Wang, M. Li, L. Zeng, Y. Li, In situ deposition of gold nanoparticles and L-cysteine on screen-printed carbon electrode for rapid electrochemical determination of As(III) in water and tea, Biosensors 13 (2023) 130.

[36] W. Pooi See, S. Nathan, L. Yook Heng, A disposable copper (II) ion biosensor based on self-assembly of L-cysteine on gold nanoparticle-modified screen-printed carbon electrode, Journal of Sensors (2011, 2011,), 230535.

[37] A. Dehnavi, A. Soleymanpour, Silver nanoparticles/poly(L-cysteine) nanocomposite modified pencil graphite for selective electrochemical measurement of guaifenesin in real samples, Measurement 175 (2021), 109103.

[38] C.A. Martínez-Huitle, M. Cerro-Lopez, M.A. Quiroz, Electrochemical behaviour of dopamine at covalent modified glassy carbon electrode with l-cysteine: preliminary results, Mater. Res. 12 (2009).

[39] D. Majer, M. Finšgar, Single-drop analysis of epinephrine and uric acid on a screen-printed carbon electrode, Biosensors 11 (2021) 285.

[40] Ž.Z. Tasić, M.B.P. Mihajlović, M.B. Radovanović, A.T. Simonović, D.V. Medić, M. M. Antonijević, Electrochemical determination of L-tryptophan in food samples on graphite electrode prepared from waste batteries, Sci. Rep. 12 (2022) 5469.

[41] D. Majer, T. Mastnak, M. Finšgar, An advanced statistical approach using weighted linear regression in electroanalytical method development for epinephrine, Uric Acid and Ascorbic Acid Determination, Sensors 20 (2020) 7056.

[42] P. Manisankar, S. Viswanathan, A.M. Pusphalatha, C. Rani, Electrochemical studies and square wave stripping voltammetry of five common pesticides on poly 3,4-ethylenedioxythiophene modified wall-jet electrode, Anal. Chim. Acta 528 (2) (2005) 157–163.

[43] S. Sultan, A. Shah, B. Khan, J. Nisar, M.R. Shah, M.N. Ashiq, M.S. Akhter, A. H. Shah, Calix[4]arene derivative-modified glassy carbon electrode: a new sensing platform for rapid, simultaneous, and picomolar detection of Zn(II), Pb(II), As(III), and Hg(II), ACS Omega 4 (16) (2019) 16860–16866.

[44] P. Borman, D. Elder, Q2 (R1) validation of analytical procedures, ICH Quality guidelines 5 (2017) 127–166.

[45] S. Pradhan, M. Bhattacharyya Banerjee, S. Biswas, N. Aliya Hamizi, D.K. Das, R. Bhar, R. Bandyopadhyay, P. Pramanik, An efficient simultaneous electrochemical detection of nanomolar epinephrine and uric acid using low temperature synthesized nano-sized copper telluride, Electroanalysis 33 (2) (2021) 383–392.

[46] W. Ren, H.Q. Luo, N.B. Li, Simultaneous voltammetric measurement of ascorbic acid, epinephrine and uric acid at a glassy carbon electrode modified with caffeic acid, Biosens. Bioelectron. 21 (7) (2006) 1086–1092.

[47] L. Luo, F. Li, L. Zhu, Y. Ding, Z. Zhang, D. Deng, B. Lu, Simultaneous determination of epinephrine and uric acid at ordered mesoporous carbon modified glassy carbon electrode, Anal. Methods 4 (2012) 2417–2422.

[48] J.X. Qiao, H.Q. Luo, N.B. Li, Electrochemical behavior of uric acid and epinephrine at an electrochemically activated glassy carbon electrode, Colloids Surf. B Biointerfaces 62 (1) (2008) 31–35.

[49] R. S, P. Abraham, A. S, A. Kumary V, Graphene-Palladium Composite for the Simultaneous Electrochemical Determination of Epinephrine, Ascorbic acid and Uric Acid, Journal of The Electrochemical Society, 166 (2019) B1321.

[50] A.A. Ensafi, M. Taei, T. Khayamian, Simultaneous determination of ascorbic acid, epinephrine, and uric acid by differential pulse voltammetry using poly(p-xylenolsulfonephthalein) modified glassy carbon electrode, Colloids Surf. B Biointerfaces 79 (2) (2010) 480–487.
[51] Y. Zhang, W. Ren, S. Zhang, Simultaneous determination of epinephrine, dopamine, ascorbic acid and uric acid by polydopamine-nanogold composites modified electrode, Int. J. Electrochem. Sci 8 (2013) 6839.
[52] S.I. Khan, K.K. Tadi, R.R. Chillawar, R.V. Motghare, Interfacing Electrochemically reduced graphene oxide with Poly(erichrome black T) for simultaneous determination of epinephrine, Uric Acid and Folic Acid J. Electrochem. Soc. 165 (16) (2018) B804–B813.
[53] U.N.O.o. Drugs, C. Laboratory, S. Section, Guidance for the Validation of Analytical Methodology and Calibration of Equipment Used for Testing of Illicit Drugs in Seized Materials and Biological Specimens: A Commitment to Quality and Continuous Improvement, United Nations Publications, 2009.